

# ON THE INITIATION OF SPIRAL WAVES IN EXCITABLE MEDIA

S. P. HASTINGS<sup>1</sup> AND M. M. SUSSMAN<sup>2</sup>

ABSTRACT. Excitable media are systems which are at rest in the absence of external input but which respond to a sufficiently strong stimulus by sending a wave of “excitation” across the medium. Examples include cardiac and cortical tissue, and in each of these examples rotating spiral waves have been observed and associated with abnormalities. How such waves are initiated is not well understood. In this numerical study of a standard mathematical model of excitable media, we obtain spirals and other oscillatory patterns by a method, simple in design, which had previously been ruled out. We analyze the early stages of this process and show that long term stable oscillatory behavior, including spiral waves, can start with very simple initial conditions, such as two small spots of excitation, and no subsequent input. For this model system, we find that random stimulation produces stable oscillations relatively often.

## 1. INTRODUCTION

Spiral and other repetitive waves in excitable media are associated with cardiac abnormalities [22, 3], cortical oscillations [11], retinal spreading depression [8], patterns in the Belousov-Zhabotinsky reaction [15], aggregations of *Dictyostelium discoideum* amoebae [7, 18], and other systems [24]. There is good theoretical work on fully formed waves [13, 14], but how they are initiated is not well understood [24]. Mechanisms which have been proposed depend either on stimulations at two separate times, [23, 24] or the medium being inhomogeneous [25, 24], or there being internal barriers with corners [1, 24]. Here we present the results of numerical computations on a standard partial differential equation (PDE) system model for such studies, the FitzHugh-Nagumo equations [4, 16, 17] which indicate that repetitive oscillations, including spirals, can be generated by an initial multi-point stimulation in the interior of a spatially homogeneous simply connected region and no further stimulation or disturbance. This possibility was ruled out over 70 years ago [22], based on hypotheses later determined to be in part unrealistic [13, 5, 6]. However to our knowledge, no one has challenged the result in [22] in print since. We have found simple stimulation patterns which lead to oscillatory behavior and which we hope are accessible in the laboratory, and we have developed some qualitative understanding of the underlying physical processes which occur in several of our examples.

---

<sup>1</sup> Department of Mathematics, University of Pittsburgh, sph@pitt.edu, <sup>2</sup> Independent Researcher, 5026 Belmont Ave, Bethel Park, PA 15102, mmsussman@gmail.com

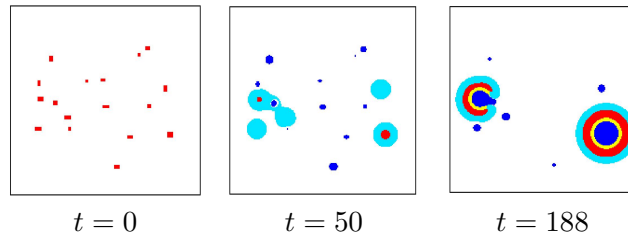


FIGURE 1. Red areas are excited and dark blue areas are refractory.

Our first efforts involved pseudo-randomly generated and positioned excited rectangles in a field otherwise at equilibrium. One such experiment is shown in Figure 1.

The  $t = 0$  case shows the set of initially excited rectangles, which will be observed to vary in size. Most of them turn out to be too small to generate an outgoing wave, and as at  $t = 50$  in Figure 1, quickly become refractory. This behavior, and others we observe as the pattern progresses, will be explained qualitatively in some detail below.<sup>1</sup>

However wave-like behavior is observed to emanate from two areas. The pattern on the right at  $t = 200$  is a typical “target” pattern that will develop into a circular expanding wave. The C-shaped wave on the left, in contrast, is observed to cause complex repetitive behavior. The generation of this wave from excited and equilibrium conditions alone, in a homogeneous simply connected region and without further intervention, is the central result of this paper.

After some introductory material, and a detailed description of the processes observed in Figure 1 we will present examples of C-shaped waves which arise from simpler configurations than this one, which we call “seeds”, that may be amenable to experimental confirmation. Some of these were obtained by successively removing cells from a spiral-generating random start, but as we gained understanding of how these worked, we were able to contrive new seeds ourselves. We also include some remarks about properties we have observed, or not observed, in our simulations and how they may relate to the size of the region being studied.

## 2. MATHEMATICAL MODELS OF EXCITABLE MEDIA

Excitable media are characterized by having three identifiable states, “rest”, “excited”, and “refractory” and by not supporting spatially homogeneous oscillations. The rest, or equilibrium, state is stable to small perturbations. A “cell”, or region, in the excited state influences neighboring cells or regions which are in the rest state by diffusion. The strength of the diffusion

<sup>1</sup>Terms such as “excited” and “refractory” will be defined in the next section.

is sufficient to move a neighboring rest state region into the excited state. An excited state soon becomes "refractory", a state in which the cell neither stimulates, nor is stimulated by, its neighbors. Refractory regions eventually return to rest, but the time spent in the refractory state is usually significantly longer than the time that a region is excited.

The simplest type of mathematical model for an excitable medium is a cellular automaton (CA) of the type described in [9], and more generally in [10]. It turns out that the models in [10] are too simple to support the behavior described in the first paragraph above, so we will not discuss them here.

The model in [22] is sometimes described as a CA, but careful reading reveals that it is more sophisticated, with continuous time, space, and state. The discussion is geometric, with waves of excitation moving around the homogeneous medium according to certain rules. From these rules it was deduced as a "theorem" that no wave exhibiting "flutter" could be initiated with just regions of rest and of excitation. By flutter the authors meant "self-perpetuating steady-state waves moving around the closed path in one direction." Rotating spiral waves are one example.

One of the rules in [22] is: "cardiac impulses, once started, spread with a constant velocity equal in all directions as far as the network continues". It is this hypothesis which was later shown to be non-physical. And it is crucial in the proof of the theorem in [22]. But [22] predated the introduction by Turing [19] of partial differential equations as viable models for such systems. Since then, studies of such models and also experiments have made it apparent that the speed of advance of a wave front in an excitable medium at any given point depends on the curvature of the wave at that point. Perhaps the first report of this was in [23]. In [13], asymptotic methods are used to show the effect, and some early experiments are in [15]. However both the theory and the experiments studied existing fully formed rotating waves. To this day, experiments generally start with a stimulus that produces an outgoing wave. Once it is fully developed, some method is used to break the wave front, which allows the ends of the wave to circle around and eventually restimulate the initial area of the wave break. In other cases, inhomogeneous media, or special types of interior obstacles, create the same effect.

Recently we found that if the very simple cellular automaton in [9] is modified in one simple way, continued activity can occur from an initial condition containing only excited and rest cells and with no subsequent disturbance. This activity seemed completely unphysical, more like "chaos" than spirals, and so we will not give details here. Nevertheless, motivated by the CA results, we felt it was reasonable to look at a system of PDE's of excitable type and see if we could produce spirals from only excited initial conditions. We succeeded in this effort, and now describe our methods and results.

**The numerical model.** As mentioned above, we did numerical experiments using the FitzHugh-Nagumo equations, which are

$$(2.1) \quad u_t = D\Delta u + au(1-u)(u-b) - v$$

$$(2.2) \quad v_t = \varepsilon(cu - v)$$

Throughout our study,

$$D = 10^{-5}, a = 0.5, c = 1.0, \varepsilon = .002,$$

while  $b$  will be chosen at or close to 0.17 in all our examples.

Our numerical calculations suggest that with our other parameters as given above, if the “threshold”  $b$  is 0.2 or higher then all solutions tend to rest. On the other hand, for  $b = 0.1$ , spirals had been seen previously, but with refractory cells present from the beginning [21]. We saw the behavior we were looking for when  $b$  was in the range from 0.165 to 0.19. We did not try to find the maximal interval in  $b$  which supported this behavior

Our computations were based on square meshes of different sizes, say  $M \times M$ . We will denote the region covered by such a mesh by  $\Omega$ . The spacial discretization was based on “cells” of size  $\Delta x = \Delta y = .005$ .<sup>2</sup> Thus, as  $M$  changed, so did the size of the domain  $\Omega$ . We chose  $u(x, y, 0)$  in each cell to be either 0 or 0.8, the latter easily being shown to be in the excited range for this model with our parameters, and we set  $v(x, y, 0) = 0$  for all  $(x, y)$ .

### 3. DETAILS OF THE STEPS LEADING TO FIGURE 1

We ran many cases of this type. For each, our pseudo-random number generator produced a set of randomly placed “spots”, which were rectangular sets of cells in the mesh with dimensions  $m \times n$ , meaning  $m$  cells along a horizontal edge and  $n$  cells along a vertical edge. Here  $m$  and  $n$  were chosen randomly in a specific range for each spot. These spots were placed well into the interior of the square  $\Omega$ . We set  $u(x, y, 0) = 0.8$  on each cell in these spots,  $u = 0$  elsewhere, and  $v(x, y, 0) = 0$  everywhere. This was the nature of our “stimulation” throughout the work described in this paper.

For boundary conditions we chose those of Neumann (no-flux) type.<sup>3</sup> In these random simulations we used square domains of between 100 and 600 mesh cells on a side. After experimentation we used spots which were between 3 and 7 cells on a side. We continued a run until the maximum value of  $u$  over the entire field was less than  $b$ , since further excitation was then impossible.<sup>4</sup> If this did not happen within a predetermined maximum number of time steps, (often 4000), then the starting configuration was saved for further study.

We extended the runs of successful trials for extended periods beyond the initial screening and in all but a few cases the wave persisted over many

<sup>2</sup>Further details of our numerical methods are given in Section 5

<sup>3</sup>See Section 5.

<sup>4</sup>This can be shown by phase plane analysis as presented below.

cycles around the region. The example shown briefly in the introduction is one of the latter cases. Before discussing it in detail, we wish to point out that for this model, it was not particularly rare for the pattern to survive to the point of apparent persistence. In a trial with  $b = 0.169$  of 1000 random choices of up to 35 spots in a  $200 \times 200$  mesh, 37 of them lasted 4000 steps, or until  $t = 2000$ . And we believe, based on some integrations for hundreds of thousands of time steps, that all of the surviving patterns in this case would have continued indefinitely. We hope in the future to examine this question for a model which bears a closer relation to a particular physical setting. The article [20] is about one such model.

To describe our results we decided to add two new states to the traditional list of “resting”, “excited”, and “refractory”, which we call “wave front” and “wave back”. These bridge the gap in the  $u$  variable between the excited and the rest and refractory states. More information is in the caption to Figure 1, and in our analysis below of the sequence of images in this figure.

Many authors have discussed the fronts and backs of waves in the context of excitable media; see [22, 24] for example. Usually, however, one or both of these are thought of as curves, separating the excited region from the others. Because our model is continuous, it makes sense for both our wave front and wave back to have significant positive area. In the fully formed wave the front is considerably wider, but in the initial stage of pattern development, when indeed the words “wave”, “front”, and “back” are somewhat misleading, this is not the case. In our analysis of our graphical results, at those stages of the development when there are not yet waves or wave fronts or backs, we will simply refer to these regions by their color.

The terms rest, excited, and refractory are not precisely defined for a continuous model, which means that the color coding, which we discuss further below, is somewhat arbitrary. However it serves to organize our description of the results of our computations. A more refined graphical presentation would result from plotting contour lines for the  $u$  and  $v$  variables, and we will give an example of this.

As the pattern evolves, both the diffusion term in (2.1), that is  $D\Delta u$ , and the other terms in both equations, referred to as either the “dynamics” or “reaction” terms, are important, but at different times and places.

In order to explain the very earliest steps in the process, we must first give a brief introduction to the phase plane for the system of ordinary differential equations obtained by dropping the diffusion term in (2.1).

**The phase plane.** We now consider the ode system

$$(3.1) \quad U' = aU(1 - U)(U - b) - V$$

$$(3.2) \quad V' = \varepsilon(cU - V)$$

Figure 2 shows the phase plane when  $a = 0.5$ ,  $b = 0.17$ ,  $c = 1$ , and  $\varepsilon = .002$ . In that figure, let  $\gamma$  denote the middle branch of the  $U$  nullcline. Since for each  $V$ ,  $U' < 0$  in the region from  $U = 0$  to  $\gamma$  and  $U' > 0$  in the

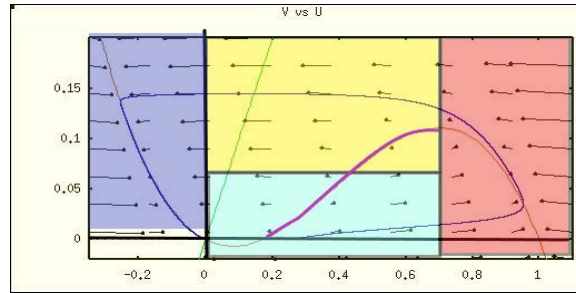


FIGURE 2. color code: red=excited ( $u \geq 0.7$ ); dark blue=refractory, ( $u \leq 0, v > 0.01$ ) light blue = wave front, ( $0 < u < 0.7, v < 0.06$ ), yellow= wave back ( $0 < u < 0.7, v \geq 0.06$ ), all else is white, referred to as rest.

region from  $\gamma$  to the right decreasing branch of this nullcline, points on  $\gamma$  are unstable equilibrium points of (3.1) when  $V$  is taken as a constant. In Figure 2 we also show a trajectory starting at  $(0.3, 0)$ , a point somewhat to the right of  $\gamma$ . Note that it passes through the colored regions in what we will call the “standard order” of states or colors:

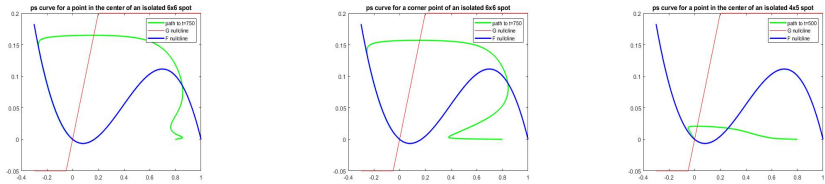
$$\begin{aligned} \text{wave front} &\rightarrow \text{excited} \rightarrow \text{wave back} \rightarrow \text{refractory} \rightarrow \text{rest} \\ &\text{or} \\ \text{light blue} &\rightarrow \text{red} \rightarrow \text{yellow} \rightarrow \text{dark blue} \rightarrow \text{white}, \end{aligned}$$

and never again leaves the rest state, since  $(0, 0)$  is an asymptotically stable equilibrium point for (3.1,3.2). In the next figure, and several further on, we consider plots of curves of the form  $t \rightarrow (u(x, y, t), v(x, y, t))$  for some specific points  $(x, y)$  in our domain, where  $(u, v)$  is a solution to (2.1),(2.2). We will refer to any curve of this sort as a pseudo-phase plane, or “PS”, curve.

The differences between PS curves and phase plane curves for (3.1),3.2) are, of course, due to the diffusion term in (2.1). If a fully developed wave crosses the point  $(x, y)$  away from any end point this wave may have, then the corresponding part of the PS curve passes through the colors in the standard order. However this is not always true near a wave tip, and it is also not always true for the seed of a developing wave, as we will see in the following section.

In Figure 3 we follow the development of two isolated spots, one larger and one smaller. This figure refers to two separate simulations, in each of which one of these spots is the only initially stimulated spot in  $\Omega$ , all else starting at equilibrium. The larger spot generates an outgoing target wave and the smaller spot decays to rest without any significant effect beyond its own neighborhood.

The small single spot case shows how a refractory region can be produced in such a way that it is not hidden behind an advancing wave, and so can



large initial spot, center    large initial spot, corner    small initial spot

FIGURE 3. In the center of the larger spot,  $u$  increases for a brief interval due to the dynamics, then decreases temporarily due to diffusion from lower  $u$  regions, but remains in the excited state until  $v$  has increased significantly. As a result the larger spot follows the standard state or color order from excited back to rest. At a corner of the large spot,  $u$  decreases into the blue region due to diffusion from below, but then the positive and negative diffusive effects from areas of higher or lower  $u$  become more balanced, allowing the reaction terms to pull this area back to the excited state. From there, all cells in the larger spot follow the normal order of states back to rest, though they may not remain there. In contrast, all points in the smaller spot are subject to greater diffusive effects from the regions where  $u$  is small than from nearby excited cells, which causes  $(u, v)$  on the PS curve to cross the  $U$  nullcline. From that point, reaction and diffusion from rest areas are acting in the same direction, with reaction now dominating and pushing  $u$  negative, and so  $(u, v)$  becomes refractory without ever entering the yellow region. This is not, therefore, the standard color order.

interact with something coming toward it. That is crucial to the process of generating patterns from initial conditions having no refractory region.

We will call a spot which, when placed on its own, does not generate any wave which reaches the boundary of a sufficiently large domain  $\Omega$  “subcritical”. This is a property which depends only on the dimensions  $m$  and  $n$  of the spot.<sup>5</sup>

It is entirely possible, and indeed important in some of our examples, that two or more subcritical spots, if placed close enough together in an otherwise empty domain  $\Omega$ , will generate a wave which reaches the boundary of  $\Omega$  no matter its size. We will point this situation out when it occurs. Moreover, we will extend our definition of the term “subcritical” to apply to any subset of the initial spots in an initial condition. Such a subset is subcritical if no

<sup>5</sup>We believe, based on our simulations, that for any given  $m$  and  $n$  there is an  $M$  such that if an  $m \times n$  spot is entirely contained in a square of side  $M/2$  centrally located within the  $M \times M$  domain  $\Omega$ , and it generates a wave which reaches the boundary of  $\Omega$ , then this wave will reach the boundary of any larger square domain containing  $\Omega$ . An  $M$  with this property therefore will be “sufficiently large” in our definition of “subcritical”.

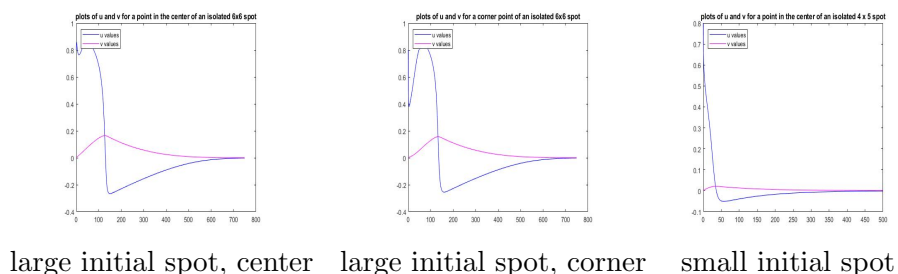


FIGURE 4. Note that the time spent in the refractory region is relatively small for the small spot.

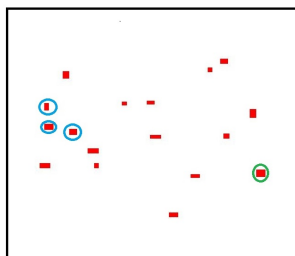


FIGURE 5. initial condition for Figure 6

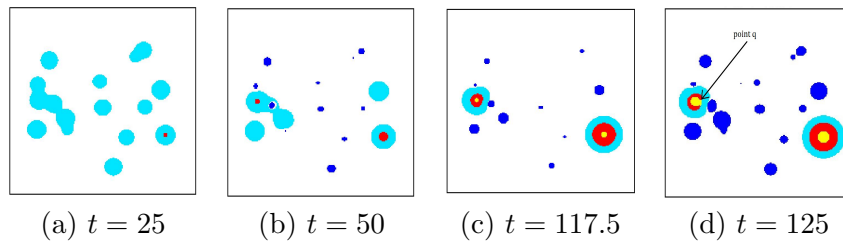
persisting wave is generated when all spots of the initial condition not in this subset are reset to equilibrium.

The behavior described in Figure 3 can also be seen in time plots of  $u$  and  $v$  at the two points being examined, as shown in Figure 4.

**Analysis of initial steps in Figure 1.** One of our goals in this analysis is to determine the relative importance of diffusion and reaction at different stages of pattern evolution. One indication of this is the degree to which a PS curve as described earlier follows a path different from a trajectory in the phase plane with the same start point. The color coding gives a crude indication of this. Many different color codes could be chosen, and we make no claim that ours is the most useful. But it did at times alert us to unusual behavior which we could then examine by plotting PS curves.

In the example of Figure 1, the pseudo-randomly chosen initial condition is shown in Figure 1(a) above, followed by intermediate positions in Figures 1 (b) and (c). More detailed behavior is shown in Figures 6, 7 and 9, and by “time” 6000 we arrived at the pattern in Figure 9(c).

Before beginning our analysis of this process, we will reprint the initial condition with some spots circled. Recall that the set of spots in its entirety was found in a pseudo-random search.

FIGURE 6. initial steps. Here  $b = 0.169$ 

In Figure 5, each of the uncircled spots develops like the small spot in Figures 3 and 4. The spot circled in green is big enough to generate its own target wave, as on the right in Figure 1. If any one of the three spots circled in blue is removed, then the remaining pair is subcritical. But all three work together to produce a  $C$ -shaped wave, also readily identified in Figure 1.

Figure 6 shows the earliest stages of the process, adding three frames to fill in some steps not shown in Figure 1. In Figure 6(a) diffusion from regions originally at rest has lowered  $u$  into light blue state in almost all of the originally excited area, despite the influence of the reaction terms, which by themselves would keep  $u$  in the excited range until the slow rising variable  $v$  had increased significantly. This can be seen also in Figures 3 and 4.

But then in much of the domain diffusion weakens, because of smaller gradients in the  $u$  variable. Absent high  $u$  variation, a blue region turns red, then yellow, then dark blue, all due to the reaction terms. Hence in Figure 6(b) we see a region on the left which has returned to the excited state, while the amount of red on the right has increased.

There are also refractory regions, in places where the original excited point was too small to produce a wave. One of these is crucial to the process we are describing. At this stage every refractory region appears because of a combination of diffusion and reaction. This important detail was described more fully in the caption to Figure 3. There has not been time for the reaction terms alone to bring an initially excited point into the refractory state, because following the standard order requires the “slow” variable  $v$  to increase significantly, at least up to the boundary between the blue and yellow regions.

The excitation pattern on the right of Figure 6 (b) is the beginning of an outgoing circular wave spreading from a center, with the dynamics dominating in the center and producing a reinvigorated red disk inside the light blue ring. (See Figures 3 and 4 for the center of the larger spot.)

In Figure 6(c), we see that yellow has appeared in the center of each excited region, producing an excited ring. We believe that in each case the yellow appears as the center cells states follow the standard order, which

includes red  $\rightarrow$  yellow, and so is due to the reaction terms. The only difference between the right and left rings is that the target pattern on the left is asymmetric, with flattened borders on the two sides, top and right, where advancement of the blue ring is blocked by the refractory regions which resulted from the smaller excited spots in those locations originally. This effect is more pronounced on the right side of this ring.

We are close to a crucial change in the configuration. The details of the transition from (c) to (d) in Figure 6 are complicated, requiring further discussion of the phase plane, and we have put these details, to the extent that we understand them, in Appendix A.

To understand Figure 6(d), look first at the excited ring on the right side of the field. This is now a circular wave, with a light blue front and a yellow back. Note that in this right target pattern, the front and the back do not meet, that is, they do not share any boundary points.

A common description of what causes repetitive patterns, perhaps originating in [22], is that the front and the back of a wave **do** meet. This is very apparent in the left side of Figure 6(d). The light blue and yellow regions meet along a curve. Moreover, there is now a point at the end of each red tip where red, yellow, and light blue come together. Such a point has been emphasized by Zykov [24] as crucial for movement of a fixed rotating spiral. He calls a point of this sort “point  $q$ ”.<sup>6</sup>

Another feature of Figure 6(d) is that the refractory regions have grown significantly. This is due to diffusion caused by the areas where  $u$  is negative and the resultant growth of those areas.

The appearance of point  $q$  makes lasting patterns possible, but nothing is guaranteed at this stage. Point  $q$  could disappear; we saw this frequently. We must continue to follow the process. And soon we have to make a decision about how to continue further. While the solution is nonzero out to the boundary of our region, the wave front does not immediately reach this boundary. We began to realize that in our smaller domains, when the front reached the boundary new effects appeared some of which are discussed below.

The remedy for this is to use a larger domain. However, computing time increases proportionally to the square of the size, and for our last example in this paper we needed domains as large as 4000x4000. Hence in some cases we ran an example until a wave was about to reach the boundary and then inserted the whole pattern into a larger field which was initially at rest. A few trials convinced us that the difference between enlarging the field before a front reached the boundary and using the larger field from the beginning was insignificant. For instance, in the example leading to Figure 1, the maximum difference in  $u$  values between running entirely on a  $601 \times 601$  domain, and starting at  $201 \times 201$  and after  $t = 150$  increasing to  $601 \times 601$ ,

---

<sup>6</sup>The exact location of point  $q$  depends on the precise definitions of the different states, which is somewhat arbitrary in a continuous model.

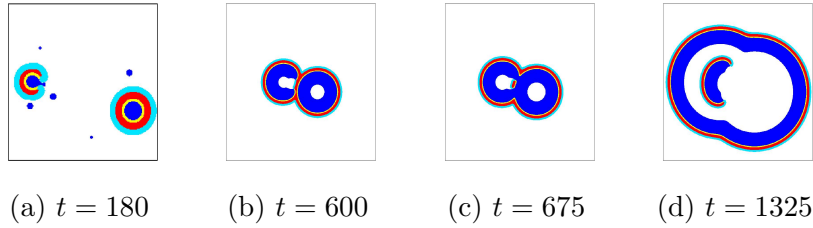


FIGURE 7. Continuation of Figure 6 to later times, and starting with (b), on a larger ( $600 \times 600$ ) field.

was less than  $10^{-8}$  at  $t = 6000$ . Continuing these two runs to  $t = 25000$ , the difference between the  $u$  values was still less than  $2 \times 10^{-8}$ .

Figure 7 continues our random example from Figure 6 (d). In Figure 7(a), the refractory region on the left has grown, due initially at least to reaction terms, and eventually the inside and outside refractory regions merge. An important influence in this breakthrough and merger of two refractory areas is diffusion, as can be seen in Figure 8, which shows a PS curve and plots of  $u$  and  $v$ . Figure 7(a) is at almost exactly the time when the graph of  $u$  turns around and heads back deeper into the refractory range. This kind up and down behavior does not occur in the  $U, V$  phase plane.

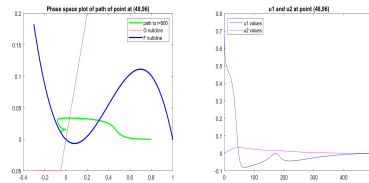


FIGURE 8. At a point where the two refractory areas merge

The excited and intermediate  $u$  regions form a  $C$  shape. On both sides of the field, the pattern is close to the boundary, so after this step we extended the range to  $600 \times 600$ , without changing  $\Delta x$  or  $\Delta y$ .

In Figure 7(b), each of the excited regions has grown, so that they are now in contact, and it looks like the  $C$  shape is going to take a bite out of the circular excited ring. This “bite” explains why the circular wave on the right does not kill off the activity on the left, as might have been expected. Since this topic is somewhat peripheral to our main message, about the earliest stages of spiral formation, we have put further details of the “bite” in Appendix C. There is also a link to a video of this process.

In Figure 7(c), the result of the intersection of the two excited regions is a new disconnected “bean-shaped” excited region with surrounding blue and

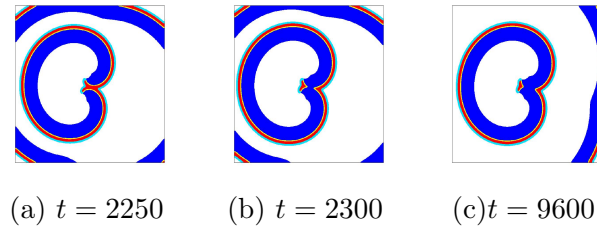


FIGURE 9. Continuation of Figure 7 at later times.

yellow bands.<sup>7</sup> Further, the wave front is, in mathematical terms, topologically equivalent to an annulus. There continue to be two points  $q$ , at the two tips of the bean.

In Figure 7 (d), a topological annulus consisting of wave front, excited wave, wave back, and trailing refractory region, has formed, while the bean from (c) has developed into a  $C$ . In this situation, we believe that what happens outside the annulus can have no effect on what happens inside, because the trailing refractory region prevents stimulation from the outside. For this to be possible in the models we are considering, it appears necessary that the domain be a certain minimum size, or larger. Once such a size has been reached, as here, no further expansion is necessary. The patterns inside do not appear to grow further.<sup>8</sup>

In Figure 9 (a), the wave front has expanded beyond the boundary. Still, however, what happens inside the  $M \times M$  domain  $\Omega$  is not influenced either by the remaining parts of the annulus still in  $\Omega$  or by the intervening regions of the boundary of  $\Omega$ . The latter is the case because of our Neumann boundary conditions. Dirichlet boundary conditions ( $u = v = 0$ ) also could not cause activity inside  $\Omega$ . From this time on, as far as the bean inside is concerned, it appears that it might as well be in an infinite domain, since as far as we have carried the computation it never reaches the boundary.

Figures 9(a),(b) show another crucial step, which can fail if the parameter  $b$  is too large or too small. The tips of the  $C$  curl around and merge, with flared out “lips” which then break off. While not so bean-shaped, the resulting wave, with a front and a back, eventually forms still another  $C$ , and the process continues.

J. Weimar [21] used a sophisticated cellular automaton model to generate a series of slides showing a similar bean generating process. Another similar process, just on a smaller field, is shown in [25]. In each of these papers the

<sup>7</sup>Here we are thinking of a string bean. Later we will see shapes more like a kidney bean, and refer to all of these simply as “beans”.

<sup>8</sup>We believe that this, and other aspects of what we are describing, arise because of the dependence of wave speed on curvature. We hope to investigate this further in the future.

waves shown started fully fledged. Our work shows that the same sort of bean generator can arise from a pattern which contains only cells which are either excited or at equilibrium. We are including patterns like those shown by others because previous researchers were studying patterns constructed to show steady rotations, while we must demonstrate that our patterns approach the same cycles as theirs.

Figure 9(c) shows the configuration after another three full cycles. Note the large time gap between Figures 9(b) and 9(c), during which the pattern has repeated itself.

#### 4. TWO FURTHER EXAMPLES

**Symmetric solutions.** After considerable experimentation, we found a class of symmetric initial configurations that would result in apparently sustained oscillations. These initial configurations have a vertical (up-down) symmetry that is maintained throughout as time progresses. The initial condition can be described as a small square  $E$  just large enough to generate an outgoing circular wave placed to the left of a long thin “barrier” rectangle  $B$ . The barrier  $B$  is thin enough that diffusion reduces its excitement faster than the dynamical terms (the terms in ( 2.1)-( 2.2) with  $D = 0$ ) can raise it. This region becomes refractory and serves to block expansion of the circular wave generated from  $E$ . The circular wave is partially extinguished as it expands to the space occupied by  $B$  and is broken into the familiar expanding C-shaped wave, as in Figure 11.

If the barrier  $B$  is short, the C-shaped wave reconnects and becomes an outgoing circular wave. If  $B$  is longer, the wave ends curl sufficiently to leave a remnant that itself may or may not remain sufficiently excited to continue to evolve.

In detail, the initial configurations can be given as two rectangles, supercritical  $E = [0.02, 0.05] \times [-0.015, 0.015]$  and subcritical  $B_\alpha [0.095, 0.1025] \times [-\alpha, \alpha]$ , for  $0 < \alpha \leq 0.5$ . Both of these rectangles are used to set  $u = 0.8$  and  $v = 0$ , values representing purely excited regions. The supercritical  $E$  rectangle is large enough that it, without  $B_\alpha$ , for any  $\alpha$ , will result in a circular outgoing target wave that allows all points to return to the equilibrium state and remain there after the wave passes. For any  $\alpha \leq 0.5$ ,  $B_\alpha$  is subcritical. Values of  $\alpha > 0.5$  have not been checked.

For  $\alpha = 0.25$ , the initial condition is shown in Figure 10. The small square region is an  $11 \times 11$  set of mesh squares, each of side length 0.005. The vertical rectangular region is  $2 \times 199$ .

Figure 11 shows the solution at four early times. At  $t = 40$ , the vertical rectangle is seen to have become less excited than initially, while the small square  $E$  has combined with the central part of  $B_\alpha$  and is becoming more excited. This introduces a horizontal asymmetry in the excited region, but still retains vertical symmetry. At time  $t = 102.5$ ,  $B_\alpha$  has become refractory,



FIGURE 10. Initial excited configuration for the symmetric case. Here  $b = 0.17$ .

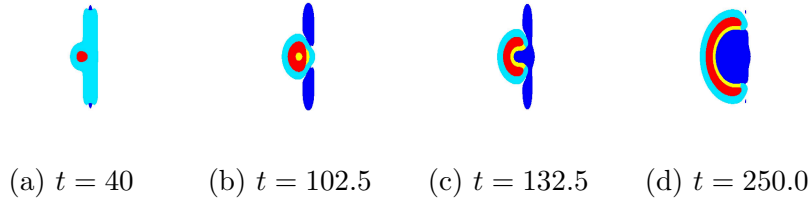


FIGURE 11. Startup

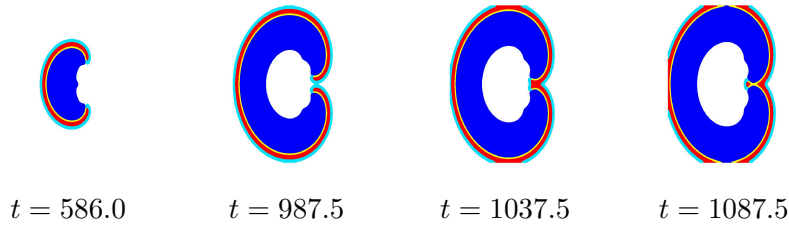


FIGURE 12. Evolution, not the same scale as Figure 11.

and the original excited region  $E$  has grown, with its outer ring excited but a yellow hole appearing in its center.

Figure 12 shows the growth of the C-shaped wave. Its ends have begun to curl because of the effect of curvature on the speed of wave advance. In Figure 12, the outer ring has closed but, because the ends have curled, at  $t = 1087.5$  the closure has caused a small excited seed to split from the outer ring. This excited seed will move toward the center of the ring, hence the term “bean generator.” By  $t = 1637.5$  (not shown), the excited seed has grown to a C-shaped wave located very close to the C-shaped wave at  $t = 586$  in Figure 12.

Figure 13 shows the history of  $u$  and  $v$  at the center point of the computational field. This point is 0.02 to the left of the initial excited region  $E$ , so it begins at equilibrium. The visual twice repetition of  $u$  between  $t = 1400$  and  $t = 2000$  supports the opinion that the solution is approaching periodicity.

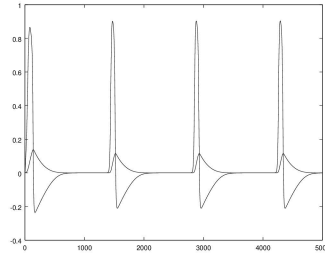


FIGURE 13. Time history of  $u$  and  $v$  at the center point of the calculational field for several repetitions.  $u$  is the higher curve,  $v$  the one with smaller peaks. Visual periodicity is apparent.

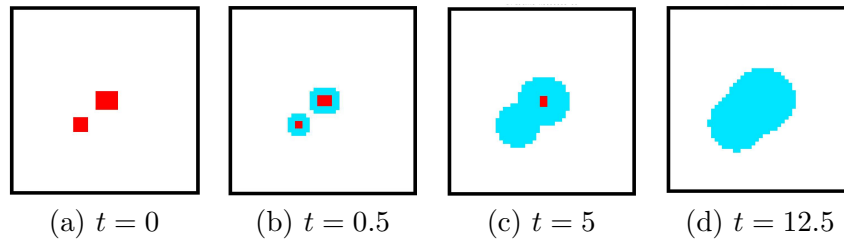


FIGURE 14. Early evolution of a pair of rectangles. Here and in the next three figures,  $b = 0.1765$ .

**An asymmetric pair of spots.** This is, in the sense of number of spots, the simplest example we have studied. Each spot is subcritical, but the pair produces a  $C$ -shaped wave. The new feature here is that a  $C$  shape of excitation is formed, but not by breaking an excited ring. Zykov's point  $q$ , as we have defined it in our model, appears before any refractory cells have appeared.

Figure 14(a) shows the initial condition. Figure 14(b) shows the field after one numerical time step, when the corresponding exact solution is smooth. Once a wave develops there will be both light blue and yellow regions, with light blue the front and yellow the back, but at this stage no yellow appears. As described before, there is a lot of light blue, caused by diffusion from the rest regions acting on the excited regions to lower the variable  $u$  before  $v$  has increased significantly. Figure 14(c) and (d) show the whole initial pair of spots pulled into light blue. There is still no sign of either yellow or a refractory region.

Figure 15(a) shows reestablishment of an excited region. Here  $v$  is still low. As described in our earlier examples, the dynamics take over and return the middle of the original larger region to the excited state. Also there is a slight flattening of the blue region on the left and this becomes

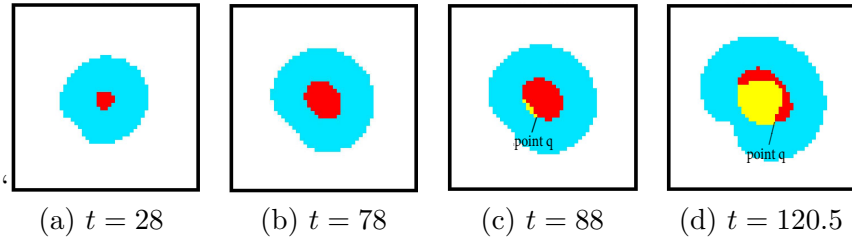


FIGURE 15. Excitation in the central region

more pronounced in 15(b). Why this occurs is not clear to us, and we give another view of it in Figure 17. More precise quantitative details may be important here.

In 15(c) and (d),  $v$  is large enough to give a small yellow region, caused by the dynamics since the points involved have made the standard transition red  $\rightarrow$  yellow. This yellow region makes the excited region concave nearby, giving the first hint of a bean-shape. By (d) the excited region has a clear  $C$ -shape, yet still, no refractory areas are evident. Our version of Zykov's point  $q$  can be identified here, at the junction of red, light blue, and yellow regions.

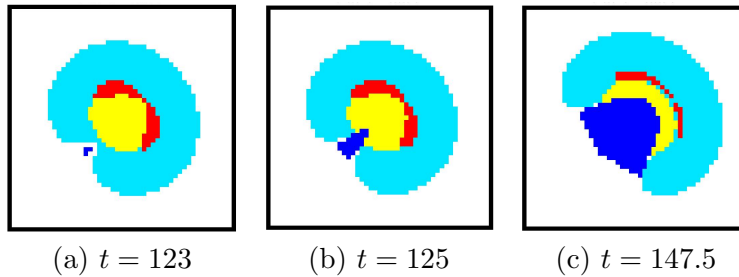
FIGURE 16. A moving  $C$ -shaped wave is established.

Figure 16 shows the establishment of a moving  $C$ -shaped wave. A refractory region (dark blue) has appeared and broken through the light blue ring. Recalling that the initial appearance of a refractory region must be caused by diffusion, at least up to the point that  $(u, v)$  cross the nullcline branch  $\gamma$ , we can expect a nonstandard PS curves for the first points which become refractory.<sup>9</sup> Hence the wave is established and begins to move upward and to the right. Eventually a bean generator of the kind in Figure 9 appears.

<sup>9</sup>One of these curves is shown in Appendix B.

When we first found an example which reached the stage of Figure 15, we were optimistic that it would survive indefinitely, but then were disappointed to see that after several generations, the bean generator failed, leaving an expanding ring which soon grew out of the field. The sensitivity of the process to the threshold parameter  $b$  became apparent. When we raised it a small amount (from 0.17 to 0.1765), we were successful for as long as we continued the simulation. Indeed, the continuity of the continuous model as a function of the parameters suggests that this will always be the case. If a nontrivial periodic pattern exists for one value of  $b$  but not for another, then we expect that between these two  $b$  values there are values where the oscillations continue for a long time but finally die out.

*Views using unfilled contours.* More information can be gleaned by looking at contour plots of  $u$  and  $v$  together. Figure 17 repeats parts of Figures 14 and 15 in contour form.

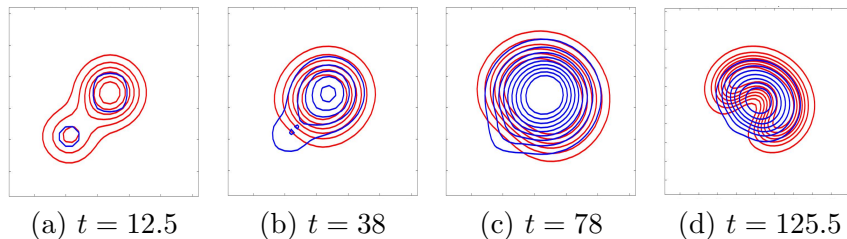


FIGURE 17. Contour versions of Figures 15(d) and 16(a),(b),(d); red:  $u$  contours, blue:  $v$  contours

Up to around  $t = 12.5$  the levels curves of  $u$  and  $v$  track each other, but later, these two sets of curves intersect in this region. Specifically, most of the trajectories of  $u$  cross most of the trajectories of  $v$ . This is seen clearly in two patches in Figure 17(d), where six levels curves of  $u$  cross six level curves of  $v$ . In the center of such a patch the  $u$  level curves are particularly close together, indicating rapid change of  $u$  in a direction crossing these curves. This area is highly unstable for the odes in (3.1),(3.2). It is sometimes called “no man’s land” [4], and is shown in a phase diagram in Appendix B, together with a sample PS curve going through this region. Zykov’s point  $q$ , two copies of which are born between Figures 17(c) and (d), is in this region. More insight into the role of these cross-hatched patches is also included in Appendix B, and a video of the process discussed in this section can be found at <https://pitt.box.com/s/dczcz1tscx6r43d2wz02vr1t1flq4ryh>.

## 5. DISCRETIZATION

The discrete form of (2.1-2.2) chosen for this study involves the standard five-point discretization of the Laplacian on a uniform, square spatial mesh. Away from boundaries, this discretization introduces a truncation error proportional to  $\Delta x^2$ , where  $\Delta x$  represents mesh spacing. Neumann conditions at the boundary are implemented by reflection, introducing an error proportional to  $\Delta x$ . As discussed below, boundary errors are small and localized near the boundary itself and do not affect conclusions reached in this paper.

An explicit Euler discretization with uniform step size is used for the temporal term. This approach introduces an error proportional to  $\Delta t$ , the step size. It also requires a limit on time step size in order to maintain numerical stability. For most of the simulations used for this paper, these limitations are not onerous.

*Boundary conditions and mesh adequacy.* In order to confirm that boundary conditions do not have a significant effect on the simulations in this paper, two simulations are carefully examined. The first is the evolution of a seed from the initial configuration with no refractory regions into an arc-shaped wavefront that closes and splits into an outwardly-moving closed wavefront and another seed in its interior (a bean generator).

Numerical experiments on square computational regions of between 200 and 600 mesh blocks of  $\Delta x = 5.0 \cdot 10^{-3}$  along each side show that the initial evolution of the seed takes place far from boundaries and is independent of boundary placement. The evolution of the arc-shaped wavefront to its closure is not affected by boundary placement so long as the wavefront does not get within about  $5\Delta x$  of the boundary. The newly created seed remains in the interior, away from the boundary, and the outwardly-moving wavefront eventually passes out through the computational boundary without influencing the interior.

A second numerical experiment compared the evolution of a seed configuration into a periodic double spiral using two different boundary conditions: Neumann and Dirichlet. The computational region is a  $10 \times 10$  square of  $2000^2$  square mesh blocks the same size as above. The relative Euclidean norm of the difference between the two solutions computed on an inner region of size  $9.75 \times 9.75$  at the same time is  $8.6 \cdot 10^{-5}$ , and still less than 5% on an inner region of size  $9.875 \times 9.875$ .

Most simulations in this paper were performed using a mesh increment  $\Delta x = 5.0 \cdot 10^{-3}$  and time step size  $\Delta t = 0.5$ . To determine that this selection is adequate to simulate solutions of (2.1-2.2), a Richardson type error analysis was performed [2]. A sequence of one-dimensional simulations of an advancing wavefront were completed using progressively finer sizings. Each simulation used half the  $\Delta x$  and a quarter  $\Delta t$  of the preceding simulation. The sequence exhibited convergence at only slightly larger than the expected 0.25 rate, justifying the original choice as within the asymptotic range.

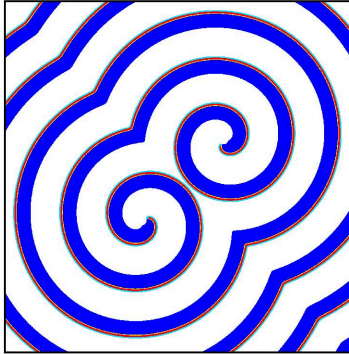


FIGURE 18. Two opposing spirals

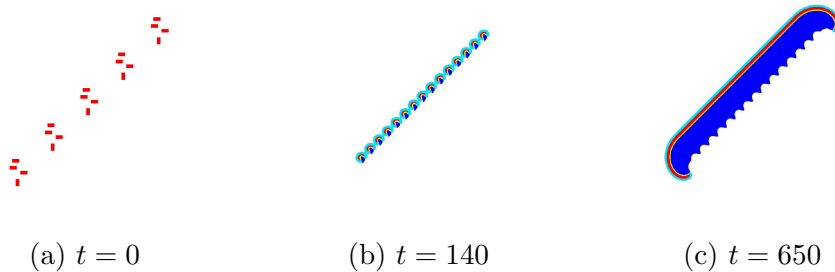


FIGURE 19. Early time configurations whose later time is illustrated in 18.

## 6. OTHER EXAMPLES, AND SOME QUESTIONS

**Opposing spirals.** We present an example of two opposing spirals surrounded by a closed curve expanding outward, as shown in Figure 18. This figure is a snapshot at problem time  $t = 10,000$  of a series of outgoing waves whose central core consists of two spirals. This situation is often observed in experiments, for example in Zykov [8], Figure 1.

In early random examples, a set of four rectangles was found to generate first a bean and then a sequence similar to the one in Figure 12. Assembling several of these sets of rectangles in a line was then found to separate the ends of the C-shaped wave sufficiently for them to curl up into spirals. For this example, fifteen identical sets of rectangles are arranged in a diagonal line as indicated in Figure 19(a). Only five of the sets of rectangles are shown, so that the details are clear.

In Figure 19(b), showing time  $t = 140$ , the beans resulting from the initial configuration are shown and in Figure 19(c), showing time  $t = 650$ , the beans have combined into a long, narrow C-shaped wave oriented at an

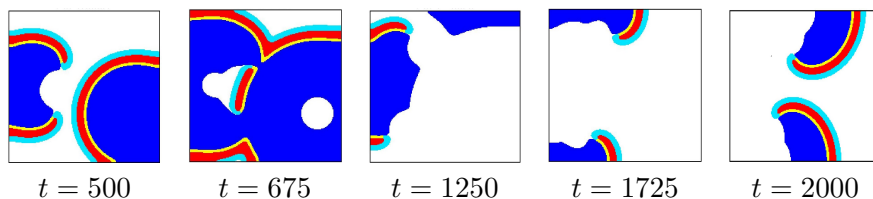


FIGURE 20. Two snakes

angle of  $\pi/4$ . The ends of this C-shaped wave curl into spirals which don't touch until after a full turn.

**A pattern where boundaries are important.** Experimental evidence showing clear spiral like behavior, with spirals of even one complete turn, is much easier to come by in chemical preparations than in neurobiological ones. For instance the well known example in [11] showed only what might be called the tip of a spiral, where as in [23], fully developed spirals were found. We expect that when it becomes possible to run such experiments on larger sections of brain tissue, more fully formed spirals will be observed.

We considered a few examples on restricted fields to see the effect of the boundary on the solution. As elsewhere in this paper, and following [11], we use Neumann boundary conditions.

Figure 20 shows results obtained using the same initial conditions of Figure 1 in a fixed field of  $201 \times 201$  cells. Thus we start from Figure 6(a).

For a while, the process is much like a cropped version of Figure 1. As before, a C-shape is produced from a bean, but the C does not have room to develop into a bean generator. As the C enlarges and moves outward, the middle part disappears across the left boundary, while the two ends survive and produce two shapes that remind us of snakes. The curling of these towards the center of the field prevents them from running off the edge.

Instead, the two snakes rotate around the edge of the square in opposite directions, and eventually collide, producing a new bean and a new C shape, in the same way that was seen for the original model in Figure 9, and when that reaches the boundary, two more snakes usually appear, or occasionally just one because the C approaches the boundary at too sharp an angle and one of its ends runs off the field. In the latter case, a single spiral develops, the only instances of this we saw. We believe that a single spiral cannot exist without reaching the boundary. None of our examples died out if the excited area at  $t = 2000$  was not very small. These "snakes" seem to evolve continually, and neither symmetry nor periodicity is evident.

The patterns in Figure 20 also resemble simulations in [26].

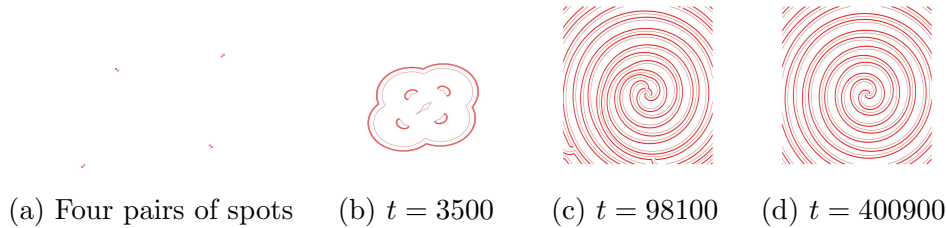


FIGURE 21. The start position, two intermediate patterns, and a final rotating double spiral, though (c) appears headed toward a triple spiral. Each pair of spots in (a) is a copy of Figure 14(a), rotated if necessary to produce an outward moving bean. The scales vary, with part (a) on a  $1001 \times 1001$  mesh, part (b) on a  $1500 \times 1500$  mesh, and parts (c) and (d) on a  $4001 \times 4001$  mesh. Here  $b = 0.1765$ .

**A two-arm spiral.** This example shows a remarkable tendency to approach a two armed spiral from earlier stages where there was no sign of spiral behavior. We are not aware of any experimental evidence for the existence of such a pattern, but it suggests an interesting mathematical question about the existence and stability of patterns for the FitzHugh-Nagumo equations on a sufficiently large domain. Our evidence is that this double spiral exists, and it has a very large basin of attraction. A video of this process can be found at <https://pitt.box.com/s/dczcz1tscx6r43d2wz02vr1t1flq4ryh>. It moves quickly at the beginning, and note the quick scale changes, but one can pause and scroll through to see the details.

**Some questions.** Based on our evidence, we have some questions for further study. For these, assume that the initial pattern of excited cells is contained in an  $n \times n$  square  $\omega$  centrally located in an  $M \times M$  square  $\Omega$ . These are questions for the PDE system 2.1, 2.2.

I. Is it the case that for each  $n$ , if  $M$  is sufficiently large then any pattern starting in  $\omega$  either tends to equilibrium uniformly in  $\Omega$  or tends to a periodically repeating pattern in  $\Omega$ .

II. Is it the case that for each  $n$ , if  $M$  is sufficiently large then no pattern approaching a periodic spiral with an odd number of arms is possible.

III. Is it the case that for any  $n$ , if  $M$  is sufficiently large then any periodic pattern is symmetric in some way?

IV. If any of the above have a positive answer, do they also hold even if refractory regions are allowed in the initial conditions?

V. Do there exist stable periodic attractors for this model?

#### ACKNOWLEDGEMENTS

We wish to thank G. B. Ermentrout, W.C. Troy, J. Tyson, and J. Weimar for encouragement to pursue this problem, and J. Weimar for providing software which he had used for the FitzHugh-Nagumo equations and which contained a module which allowed for randomization with excited and refractory cells. While we eventually used different software, it was randomization, using only excited cells, which led to success once proper parameters had been found.

We also wish to thank the Center for Research Computing at the University of Pittsburgh for the use of its facilities during this project, and R. Roskies for suggesting and facilitating this assistance.

#### REFERENCES

- [1] Agladze, K., Keener, J. P., Müller S. C. & Panfilov, A. V. Rotating spiral waves created by geometry. *Science* **264**, 1746–1748 (1994).
- [2] Atkinson, K. E., “An introduction to numerical analysis,” John Wiley and Sons, New York, 1989. ISBN 0-471-62489-6.
- [3] Davidenko, J. M, Pertsov, A.V., Salomonsz, R., Baxter, W. & Jalife, J. Stationary and drifting spiral waves of excitation in isolated cardiac muscle. *Nature* (London)**355**, 349–351 (1992).
- [4] FitzHugh, R. Impulse and physiological states in models of nerve membrane. *Biophysics J.* **1**, 445-466 (1961).
- [5] Foerster, P., Müller, S. C. & Hess, B. Curvature and propagation velocity of chemical waves, *Science* 241 (1988) 685-687.
- [6] Foerster, P., Müller, S. C. & Hess, B. Critical size and curvature of wave formation in an excitable medium, *Proc. Natl. Acad. Sci. USA* **86**, 6831-6834 (1989) .
- [7] Gerisch G. 1971 Periodische Signale steuern die Musterbildung. *Zellverbänden.Naturwissenschaften* **58**, 430–438 (1971).
- [8] Gorelova, N. A. & Bures J. Spiral waves of spreading depression in the isolated chicken retina. *J Neurobiol* **14**, 353–363 (1983).
- [9] Greenberg. J. M. & Hastings, S. P. Spatial Patterns for Discrete Models of Diffusion in Excitable Media. *SIAM Journal on Applied Mathematics.* **34**, 515–523 (1978).
- [10] Greenberg, J. M., Greene, C. & Hastings, S. P. A combinatorial problem arising in the study of reaction-diffusion equations. *SIAM J. Algebr. Discrete Methods* **1**, 34–42 (1980).
- [11] Huang, X, Troy, W. C., Yang, Q. , Ma, H., Laing, C., Schiff, S. J., & Wu, J-Y. Spiral waves in disinhibited mammalian neo-cortex. *J. Neurosci.* **24**, 9897-9902 (2004).
- [12] Izhikevich, E. M. and R. FitzHugh, *Scholarpedia*, 1(9):1349, (2006)
- [13] Keener, J. A. Geometrical theory for spiral waves in excitable media. *Siam J. Appld. Math.* **46**, 1039-1056 (1986).
- [14] Keener, J. & Tyson, J. Singular perturbation theory of traveling waves in excitable media (a review) *Physica D*, **32**, 327-361 (1988).
- [15] Muller, S., Plesser, T. & Hess, B. The structure of the core of the spiral wave in the Belousov-Zhabotinsky reaction, *Science*, **230**, 661-663 (1985).
- [16] Nagumo, J. An active line using Esaki diodes. *Inst. Elec. Commun. Engrs. Japan Professional Group on Nonlinear Circuit Theory Rept.* (1961).
- [17] Nagumo, J., Arimoto, S. & Yoshizawa, S. An active pulse transmission line simulating nerve axon. *Proceedings of the IRE* **50**, 2061-2070 (1962).
- [18] Sawai S., Thomason P. A. & Cox E. C. An autoregulatory circuit for long-range self-organization in Dictyostelium cell populations. *Nature* **433**, 323–326 (2005).

- [19] Turing, A. M. The chemical basis of morphogenesis. *Philosophical Transactions of the Royal Society of London. Series B, Biological Sciences.* **237**, 37–72 (1952).
- [20] J. R. Weimar, J. J. Tyson, L. T. Watson, Diffusion and wave propagation in cellular automaton models of excitable media, *Physica D Nonlinear Phenomena*, 55 (1992), 309-327.
- [21] Weimar, J. Cellular Automata for Reactive Systems, Doctor of Science Thesis, Universite Libre de Bruxelles Faculte des Sciences, Service de Chimie Physique, 1995.
- [22] Wiener, N. & Rosenblueth, A. The mathematical formulation of the problem of conduction of impulses in a network of connected excitable elements, specifically in cardiac muscle. *Arch. Inst. Cardiol. Mex.* **16**, 205-216 (1946).
- [23] Winfree A.T. Rotating chemical reactions. *Sci. Am.* **230**, 82–95(1974).
- [24] Zykov, V. S. Spiral wave initiation in excitable media. *Philosophical Transactions of the Royal Society A* **376**, <http://doi.org/10.1098/rsta.2017.0379> (2018).
- [25] Zykov V. S., Krekhov A. & Bodenschatz E. Fast propagation regions cause self-sustained reentry in excitable media. *Proc. Natl Acad. Sci. USA* **114**, 1281–1286 (2017).
- [26] Zykov, V. S., Krekhov A. & Bodenschatz, E. ,Geometrical factors in propagation block and spiral wave initiation, *Chaos* **27** 093923 (2017); <https://doi-org.pitt.idm.oclc.org/10.1063/1.499947> (2017)

## 7. APPENDIX

**A.** We now present further details of the transition from (c) to (d) in Figure 6. In Figure 22 (a) and (c) are the same as (c) and (d) in Figure 6 respectively, while (b) is at an intermediate time. Specifically, (b) shows the first time in the numerical simulation when yellow appears on the outside of the leftward red ring. Looking at Figure 6 (a), we ask: was the isolated yellow cell in (b) red or blue in (a)? Note that both red and blue border on yellow, and a standard order would allow only the transition red  $\rightarrow$  yellow. We could of course identify that cell in (a), but plotting a PS curve is more informative. The PS curve passing through that yellow point is shown in Figure 23. This curve does not quite reach the excited region, so the transition we asked about is from blue to yellow. While this statement is highly depending on our color code, the PS curve in Figure 23 clearly shows that diffusion is the dominant factor on this cell at the time when the solution enters the yellow zone. At this stage, therefore, it is not accurate to call the yellow and blue regions fronts or backs.

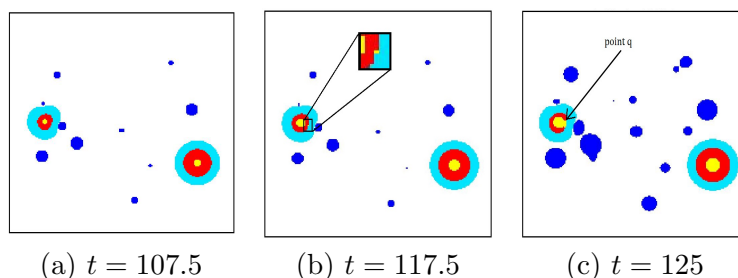


FIGURE 22. Added detail in Figure 6

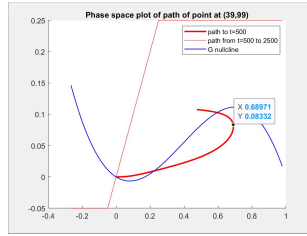


FIGURE 23. PS curve through isolated yellow cell in Figure 22(b).

B. This figure is a further detail of the example in Figure 14.

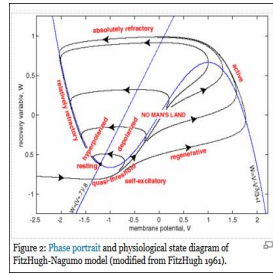
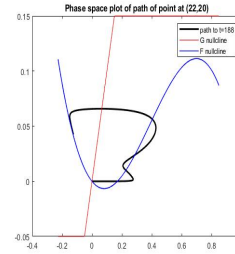


Figure 2: Phase portrait and physiological state diagram of FitzHugh-Nagumo model (modified from Fitzhugh 1961).



(a) From [12]. Notice “no-man’s land”. (b) PS curve from a patch in Figure 17

C. In Figure 7 (b) we described what happens when a  $C$ -shaped wave meets a circular wave as a “bite”. In the Figures 24, 25 we show details of this bite. Observe that as the level curves of  $u$  (red) of each pattern meet, they merge, in ways that end up dividing the outer level curves of the incoming target pattern into three sections, the middle of which has joined the inner red band of the  $C$ , beginning the formation of a bean. The inner red bands of the target pattern follow and a middle section of these splits off to complete a well formed bean, ready to move away and turn into a new  $C$ . The major areas to examine are the two cross-hatched patches at the tips of the  $C$ . Since they both survive, a new bean is born. A video of this process can be found at <https://pitt.box.com/s/dczcz1tscx6r43d2wz02vr1t1flq4ryh>

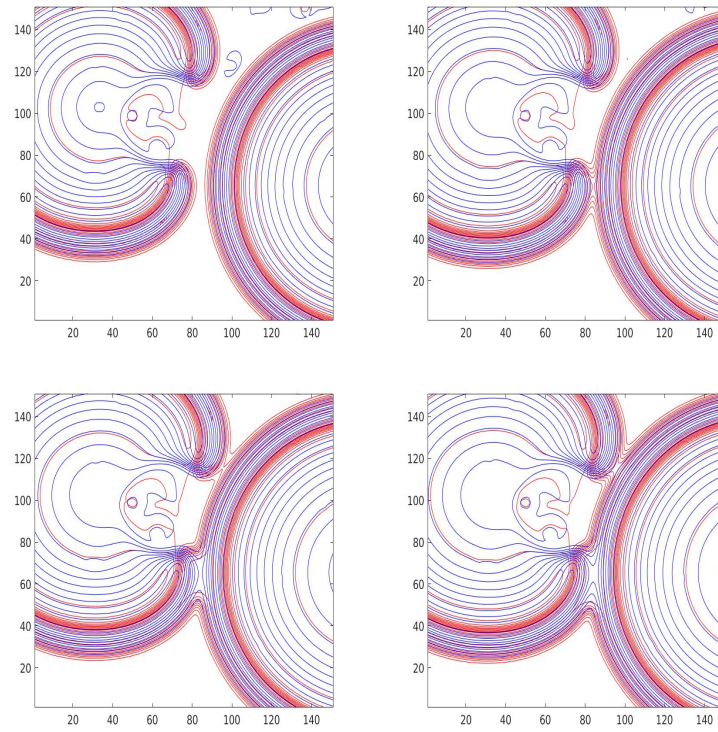


FIGURE 24. initial steps

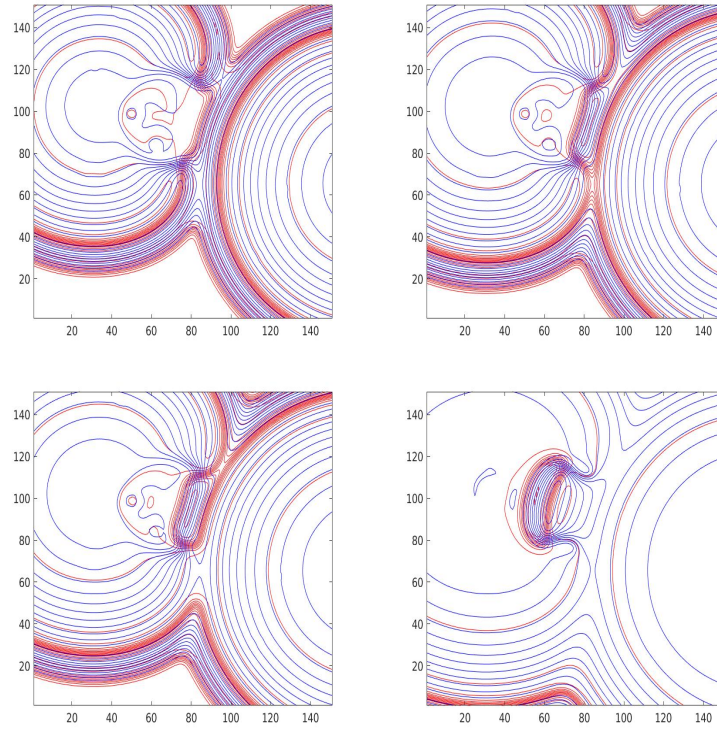


FIGURE 25. final steps

**D.** Additional input data.

In all computations using the spots below,  $dx = dy = .005$ . The first example in section 4 used a finer mesh, and its details are in that section.

For the example shown in Figure 1 there were four spots of importance. All others could be omitted and the result would be the essentially the same after 400 steps. (We did this experiment.) The initial mesh was of size  $201 \times 201$ , and the nonzero initial conditions were as follows. Here  $(a..b, c..d)$  denotes the spot with corners  $(a, c), (a, d), (b, c), (b, d)$ , where a,b,c,d are mesh indices of cells with physical corners (a dx, c dy), etc.

$$\begin{aligned} u(46..50, 96..99) &= 0.8 \\ u(30..35, 100..104) &= 0.8 \\ u(30..32, 117..120) &= 0.8 \\ u(166..171, 62..67) &= 0.8 \end{aligned}$$

These initial conditions were also used to produce Figure 20, which remained a  $201 \times 201$  mesh throughout.

For the second example in Section 4, which started on a  $51 \times 51$  domain, the nonzero initial conditions were

$$\begin{aligned} u(18..21, 18..21) &= 0.8 \\ u(24..29, 24..28) &= 0.8 \end{aligned}$$

For the example in Section 6 to produce Figure 21, which started on a  $1001 \times 1001$  domain, the nonzero spots were

$$\begin{aligned} u(215..218, 215..218) &= 0.8 \\ u(221..226, 121..125) &= 0.8 \\ u(749..752, 235..238) &= 0.8 \\ u(741..746, 241..245) &= 0.8 \\ u(375..378, 475..478) &= 0.8 \\ u(381..386, 481..485) &= 0.8 \\ u(115..118, 528..531) &= 0.8 \\ u(121..126, 521..525) &= 0.8 \end{aligned}$$